Journal of Institute of Science and Technology, 30(2), 115- 125(2025)
ISSN: 2467-9062 (print), e-ISSN: 2467-9240
https://doi.org/10.3126/jist.v30i2.84888

Research Article

PLANT-MEDIATED ZINC OXIDE NANOPARTICLE AND COPPER DOPED ZINC OXIDE NANOCOMPOSITE FOR PHOTOCATALYTIC DEGRADATION OF METHYLENE BLUE DYE

Pratikshya Pokhrel*[1], *Armila Nyachhyon Rajbhandari*[1]
[1]*Central Department of Chemistry, Tribhuvan University, Kirtipur, Kathmandu, Nepal*
**Correspondence: armila.rajbhandari@cdc.tu.edu.np*

***(Received:** September 27, 2025; **Revised:** November 30, 2025; **Accepted:** December 2, 2025)*

ABSTRACT

Green synthesis of zinc-oxide (ZnO) nanoparticles and copper-doped zinc oxide (Cu-ZnO) nanocomposites were carried out by treating zinc nitrate and copper nitrate precursors with aqueous extract of *Cinnamomum camphora* leaves powder. X-ray diffraction spectroscopy (XRD), Fourier transform infrared spectroscopy (FTIR), Scanning electron microscopy (SEM), and UV-visible spectrophotometry have been used to characterize the prepared materials. XRD analysis showed that both materials are crystalline in nature. The average crystallite size of ZnO and Cu-ZnO was found to be 21 nm and 17.51 nm, respectively. The FTIR spectra displayed clear bands of ZnO at 508.1 cm^{-1}. The SEM image demonstrated crystalline circular patch like morphology for both nanoparticles and the UV-visible spectra displayed a characteristic absorption band at 378 nm for ZnO and 382 nm for Cu-ZnO. The synthesized ZnO nanoparticles and Cu-ZnO nanocomposites have been used to degrade methylene blue (MB) under UV light. Cu-ZnO nanocomposites showed 98 % MB degradation within 240 minutes at pH 10 while only 90 % MB dye was degraded by ZnO nanoparticles. Results revealed that the optimum catalyst dose was 30 mg and dye concentration was 5 mg/L along with 0.4 mL of 1% H_2O_2. In this study, it has been demonstrated that Cu-doped ZnO displayed excellent photocatalytic efficiency towards degradation of dye within a short period of time even in low concentration.

Keywords*: Cu-ZnO, Green synthesis, Methylene blue, Photocatalytic degradation, ZnO*

INTRODUCTION

Dye pollution is a serious global problem primarily from the textile industry, where synthetic dyes and chemicals are released as toxic effluents into water and pose significant health risks to humans (Alharthi *et al*., 2020) through contamination of drinking water, irrigation, and food chain. The effluent dyes are persistent in the environment and can cause health issues such as cancer, skin diseases, respiratory problems, and damage to various organs (Hussein *et al*., 2012). Some of the common dyes that have been used are methylene blue (MB), rhodamine B, methyl orange, and indigo. Similarly, dyes can obstruct sunlight penetration and slow down the rate of photosynthesis in aquatic life as well. Therefore, dye concentrations must be reduced from industrial waste to a safe level or eliminated before disposing into mainstream (Cai *et al*., 2017). MB is a cationic dye (Sahu *et al*., 2020; Khan *et al*., 2022) with a molecular formula: $C_{16}H_{18}N_3ClS$, showing the maximum absorption at 609-668 nm wavelength of light (Ramsay *et al*., 2007). These days, nanomaterials have been used to degrade cationic dyes.

Depending on the size, morphological structure, and other characteristics, nanomaterials can be classified into several categories. These categories include metal nanoparticles, carbon-based materials, semiconductor-based materials, polymer-based materials, and lipid-based materials (Koutavarapu *et al*., 2020). The metal-based nanoparticles consist of various metal oxides, such as oxides of iron, zinc, titanium, gold, and silver (Bratovcic, 2019). Among those metal oxides, ZnO is a promising contender in the biomedical sector. In addition, because of their simplicity of synthesis, non-toxicity, biocompatibility, and biosafety, zinc oxide nanoparticles are preferred for biomaterial applications (Ashwini *et al*., 2021a). Furthermore, ZnO is a semiconductor having a significant band gap of around 3.37 eV and can be used as photocatalyst for dye degradation. ZnO is one of the most commonly used photocatalysts (Davar *et al*., 2015) because of its advanced oxidation properties.

Nevertheless, ZnO has some limitations as a photocatalyst, such as the quick recombination efficiency of charge carriers, such as electrons and holes, that are activated by ultraviolet light when the energy of photon exceeds the band-gap energy (Xu *et*

al., 2017; Shanmugam *et al*., 2018). Hence, in this study, we prepared ZnO NPs and modified it by doping copper in the ZnO matrix to eliminate the limitations, like recombination of charge carriers. The plant-mediated ZnO and Cu-ZnO nanoparticles exhibited highly efficient photocatalytic degradation even at low concentrations within a short time.

MATERIALS AND METHODS

Materials

Leaves of *Cinnamomum camphora* have been collected from the Tribhuvan University premises, Kirtipur, Nepal. UV-Visible Spectrophotometer **(**AB1908003, Electronics India), XRD (Bruker D2 Phaser, Bruker, Germany), and SEM (Zeiss, Germany) have been used for the physicochemical characterization of the zinc oxide nanoparticles and copper doped zinc oxide nanoparticles. Zinc nitrate hexahydrate [$Zn(NO_3)_2.6H_2O$] and Copper(II) nitrate trihydrate [$Cu(NO_3)_2.3H_2O$] have been purchased from Merck life science private limited, Sodium hydroxide (NaOH) was purchased from Central Drug House Private Limited. Methylene blue was procured from Sigma, Aldrich. The UV cabinet of the model number BLE-8T254 from Spectronics Corp, Westbury New York has been used as a UV light irradiation source. Two lamps were enclosed in the UV cabinet of 8W each.

Extract Preparation

The leaves of *C. camphora* were cleaned, dried, and crumpled into powder. Exactly 20 g of leaf powder was placed in 500 mL of distilled water and boiled so as to obtain the extract. Thus, obtained extract was cooled to room temperature and then filtered. The extract was stored at 4°C for further use.

Green Synthesis of Nano Materials

15 mL of the leaf extract was mixed with 25 mL of 0.1 M of zinc nitrate hexahydrate solution. Then it was heated to 70°C for 2 hrs at pH 9. After that, it was cooled to room temperature and centrifuged for 20 minutes at 9000 rpm. Then it was dried. The remaining pellet was rinsed three times with distilled water and dried at 90°C. It was ground to fine powder using a pestle and mortar. Powder was calcined at 400°C for 2 hrs. For the synthesis of copper doped zinc oxide nanoparticles, 100 mL 0.002 M copper nitrate solution and 100 mL 0.02 M zinc nitrate hexahydrate solution were mixed together and then 150 mL of plant extract was added to it. The solution was well mixed and pH 9 was maintained by using NaOH. The solution was stirred for 2 hrs at 70°C. Then it was cooled to room temperature and centrifuged for 20 minutes at 9,000 rpm. It was dried in an oven at 90°C. The dried material was then ground to fine powder using mortar and pestle. The obtained powder was then calcined at 400°C for 2 hrs.

Physicochemical Characterization

These materials were characterized by different techniques such as X-ray diffraction (XRD), Scanning electron microscopy (SEM), Fourier transform infra-red spectroscopy (FTIR), Ultraviolet-Visible spectrophotometry.

Dye Degradation Study

As prepared materials were then applied for the degradation of dye pollutant. Here, methylene blue (MB) has been used as model pollutant. The dye degradation percentage was calculated by using equation 1:

$$Degradation\ (\%) = \frac{C_O - C_t}{C_O} \times 100 \quad \ldots (1)$$

Where,

C_O = initial concentration

C_t = final concentration after time t

RESULTS AND DISCUSSION

In this study, white colored ZnO and bluish white colored Cu-ZnO materials were obtained.

XRD Analysis

The XRD pattern of as prepared ZnO and Cu-ZnO is presented in Figures 1 (a) and (b), respectively. In Figure 1(a), sharp diffraction peaks at position 31.49°, 34.23°, 36.06°, 47.26°, 56.41°, 62.58° and 67.84° 2θ having (1 0 0), (0 0 2), (1 0 1), (1 0 2), (1 1 0), (1 0 3) and (112) planes, respectively which resembles to ZnO according to JCPDS card No. 89-7102. Khalid *et al*., (2022) have also reported such peaks. These sharp diffraction peaks indicate the crystalline state of the materials.

Figure 1(b) shows the diffraction peaks of Cu-ZnO. Herein, all the peaks are similar to the peaks observed in ZnO in addition to a distinct peak observed at 38.35° 2θ degrees, which belongs to the plane (111) and is assigned to Cu, according to JCPDS card No. 05-0661. Similar type of peak was also reported in literature (Modwi *et al*., 2018). A slight shift of ZnO peak accounting for CuO fused on ZnO wurzite lattice was observed. These XRD pattern indicated that Cu get doped in ZnO.

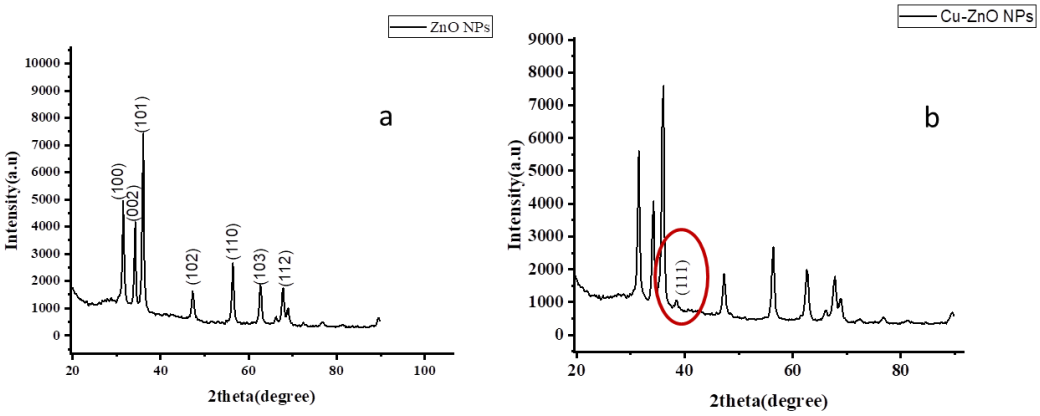

Figure 1(a). XRD of ZnO, (b) XRD of Cu-ZnO.

The average crystalline size of the synthesized materials was determined by using Scherer's equation (2)

$$D = \frac{K\lambda}{\beta \cos\theta} \qquad \ldots (2)$$

Where, D is crystal size (nm), K is the Scherrer constant (around 0.9), λ is the wavelength of XRD used, β is full width half maximum (FWHM) of a diffraction peak in radians and θ is Bragg's angle. The crystallite size of ZnO was measured to be 21 nm and Cu-ZnO was 17.51 nm. It is in agreement with the reported value of 22.26 nm (Modwi *et al*., 2018) and 17.49 nm of Cu-ZnO (Khan *et al*., 2018). Hence, the obtained materials are said to be nano in size.

SEM Analysis

The SEM image of ZnO nanoparticle is shown in Figure 2. In Figure 2(a), one can see the small, rounded shaped nanoparticles which are almost uniform in size. Similarly, SEM picture of Cu-ZnO nanocomposite is displayed in Figure 2(b). The morphology of Cu-ZnO was also observed to be nano in size with circular shape. However, some sheet-like structures are also seen in ZnO matrix, which is highlighted by red circle in Figure 2(b). The observed sheet-like morphology suggests structural modification of ZnO matrix upon copper doping. This indicates the doping of Cu particles inside the ZnO matrix.

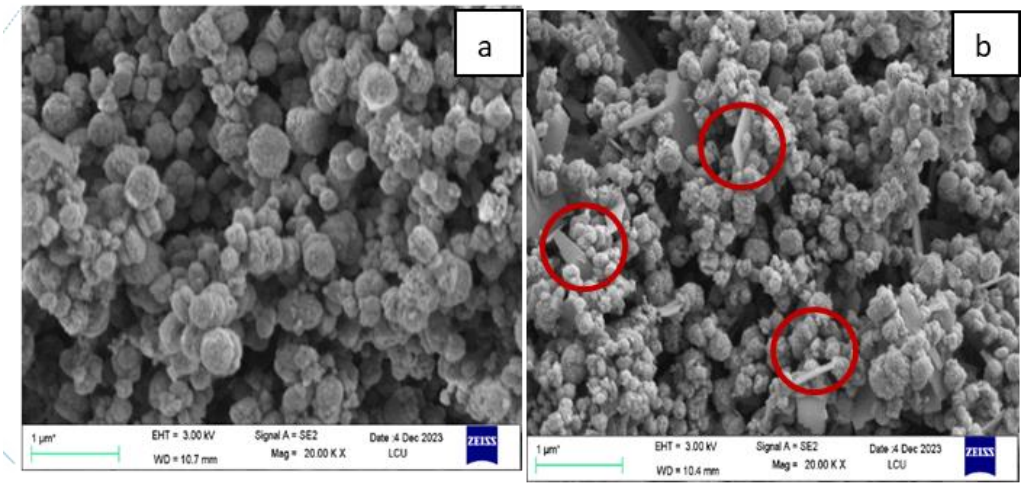

Figure 2: SEM image of (a) ZnO nanoparticles (b) Cu-ZnO.

FTIR analysis

The functional group analysis of the prepared materials was investigated by FTIR spectroscopy and spectra are displayed in Figure 3.

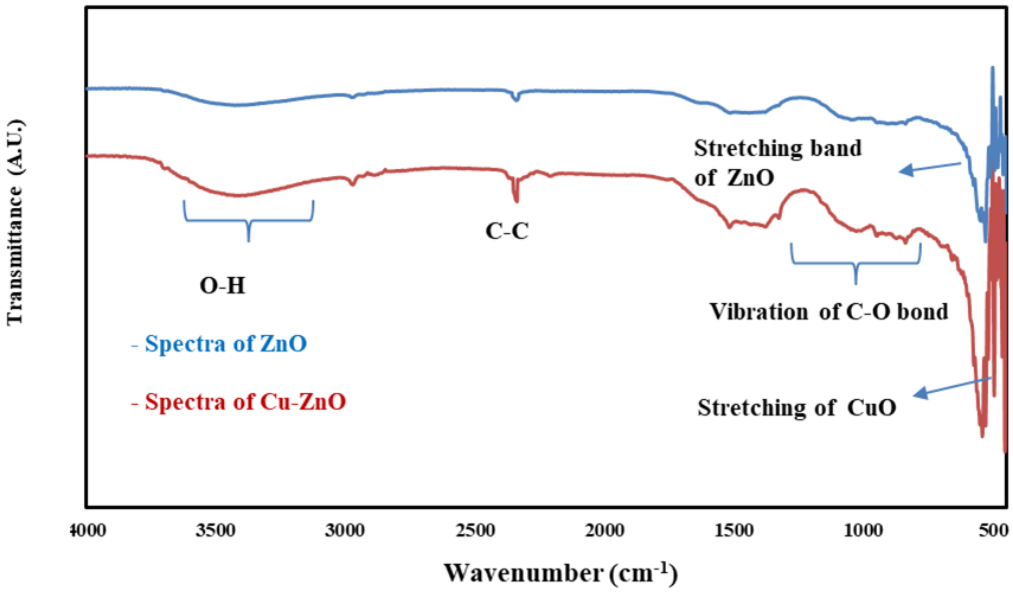

Figure 3. FTIR Spectrum of ZnO and Cu-ZnO.

The spectra of ZnO and Cu-ZnO were recorded in the range of 4000 cm^{-1} to 450 cm^{-1} wave number. In both samples, major bands were obvious at around 500 cm^{-1} to 600 cm^{-1} (Bhuyan *et al.*, 2015). The IR band at 508.01 cm^{-1} was allocated for ZnO. Similarly, weak and broad bands around 3420 cm^{-1} and 3432 cm^{-1} were assigned for hydroxyl groups. Peaks at 3100 to 3500 cm^{-1} are also attributed to O-H stretching bond in the literature (Suwanboon *et al.*, 2013). Very weak signals between 2300 cm^{-1} to 2400 cm^{-1} were due to the carbon to carbon stretching vibration (Malarkodi *et al.*, 2014). Other important signals at 1400 cm^{-1} to 1800 cm^{-1} are allocated to C-C and C-O vibrations. These vibrations may be due to the presence of organic substances existing in leaf extract. Similar bands are also observed in spectrum of Cu-ZnO. However, a band at 541.20 cm^{-1} is seen in spectrum of Cu-ZnO which was assigned to CuO. Similarly, Zn-O vibration was found around 509 cm^{-1} in both spectra. Hence, it was proved to be the existence of CuO along with ZnO (Viorica *et al.*, 2019). A similar type of stretching band of CuO at 542 cm^{-1} was also reported in literature (Shanmugam *et al.*, 2018).

UV-Visible Spectrophotometry

UV spectra (Figure 4) of ZnO nanoparticles and Cu-ZnO nanocomposites were also recorded to understand the assimilation of Cu in ZnO matrix. Absorbance is plotted against wavelength in nm. It was observed that ZnO nanoparticles displayed their characteristic absorption peak at 378 nm. Such peak is also assigned for ZnO by Khalid *et al.* in literature (Khalid *et al.*, 2022). Similarly, a clear absorption peak of Cu-ZnO nanocomposite was perceived at 382 nm which was supported by the study given by Gaurav *et al.*, (2019). Position of absorption band of Cu-ZnO was detected to be slightly shifted towards visible region. Such a bathochromic shift in absorption edge specifies the doping of Cu ions in ZnO matrix. It is a clear indication of Cu impurity in ZnO matrix. It is seen as a shift of spectra on behalf of both excitation and emission in the visible region.

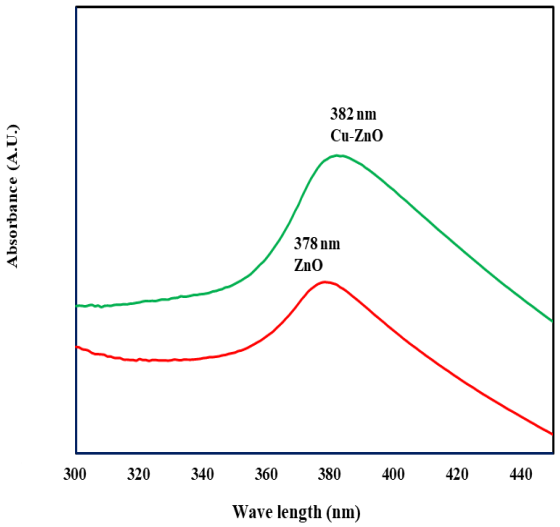

Figure 4. UV-Visible spectra of ZnO and Cu-ZnO.

The optical band gap ZnO nanoparticles and Cu-ZnO nanocomposite was estimated by using Tauc's plot (Figure 5) by extrapolating the straight line of $(\alpha h\nu)^2$ versus energy (eV) graph. The band gap energy 3.0 eV and 2.8 eV was obtained for nanoparticle and Cu-ZnO nanocomposite, respectively.

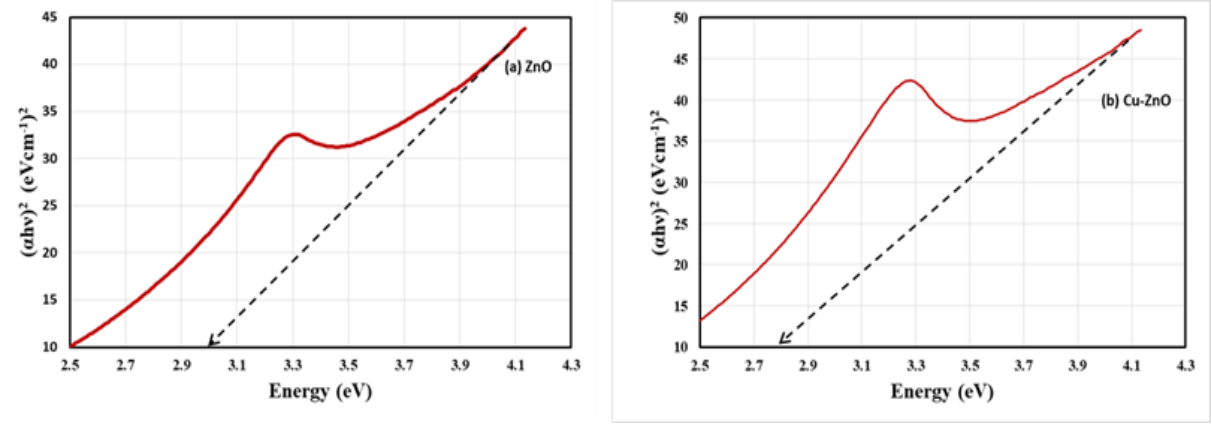

Figure 5. Tauc's plot for optical band gap of (a) ZnO nanoparticles and (b) Cu-ZnO nanocomposites.

The band gap energy of ZnO is in agreement with literature value 3.27 eV (Blažeka *et al.*, 2022) while band gap energy value of Cu-ZnO was found to be narrower than pure ZnO value. The introduction of Cu impurities in the nanocomposites narrowed the band gap to 2.8 eV which is less than the literature value of 3.25 eV mentioned in the similar work (Gaurav *et al.*, 2019). This narrowing of band gap became prominent as Zn^{2+} is gradually substituted by Cu^{2+} in the matrix of the materials and systematically increased the number of oxygen vacancies due to their ion radii and electronegativity (Yusof *et al.*, 2018). Here, the impurities created a special defect, which stimulates the Fermi level to rise towards conduction band (Ghosh *et al.*, 2015).

Photocatalytic Dye Degradation of MB

Photocatalytic efficiency of ZnO nanoparticles and Cu-ZnO nanocomposites were examined by studying the degradation of MB using UV light irradiation in different conditions. Here, MB is used as model dye. Different degradation parameters have been studied and results are presented in Figure 6.

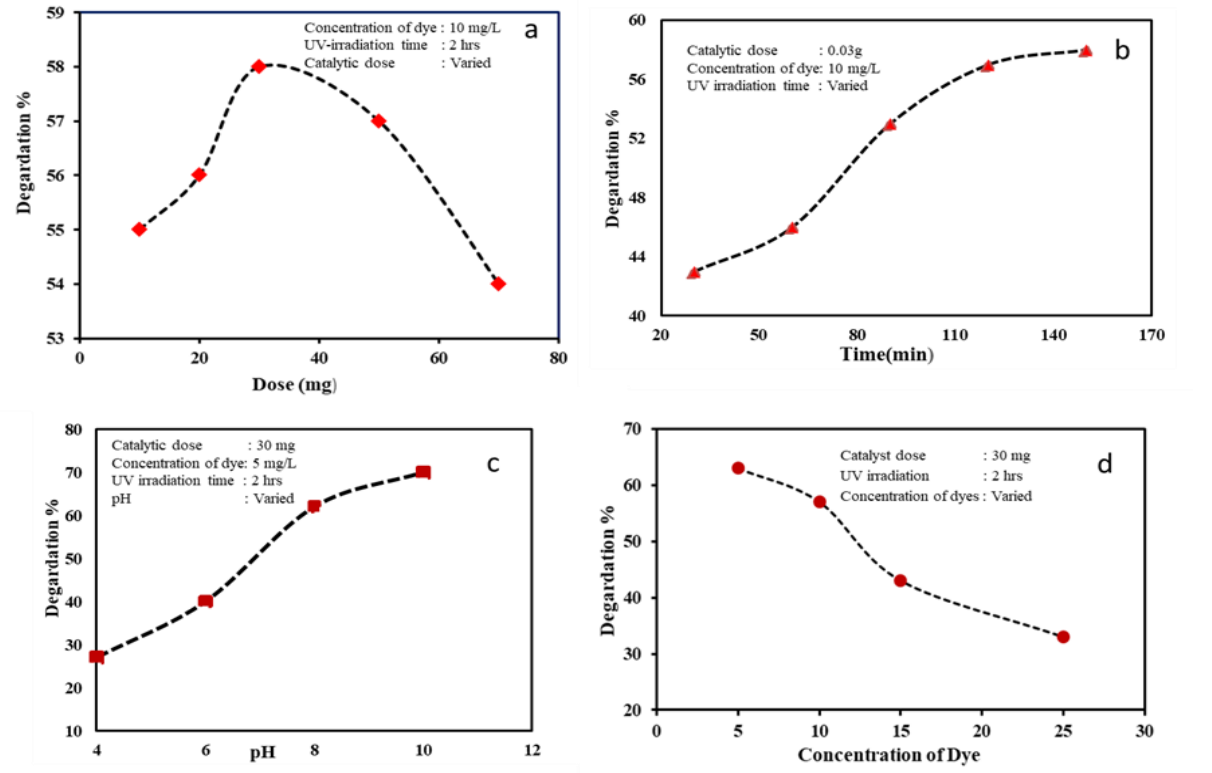

Figure 6: (a) Degradation % as a function of ZnO catalyst dose (mg), (b) Degradation % as a function of time (min) in the presence of ZnO catalyst, (c) Degradation % as a function of pH in the presence of ZnO catalyst, (d) Degradation % as a function of concentration of dye in the presence of ZnO catalyst.

Effect of Catalyst Dose in Dye Degradation

Figure 6 (a) shows 55 % MB degradation when 10 mg ZnO was used in photocatalysis. When ZnO dose was amplified, the degradation percent was improved. Percent degradation of MB using ZnO NPs were observed to be 56%, 58%, 57%, and 54% for the dose of 20, 30, 50 and 70 mg, respectively. The highest degradation percent was found when 30 mg of catalyst was used. It may be due to an increase in number of electron-hole pairs. Hence, the optimum dose was 30 mg. The high catalyst dose causes turbidity, which hinders the irradiated light in the solution. This reduces the rate of the reaction in solution. High catalyst dose may create an agglomeration of ZnO which reduces effectiveness of ZnO.

Effect of Irradiation Time in MB degradation

Figure 6 (b) shows a gradual upsurge of percent degradation with irradiation time. The 43% degradation was observed at 30 minutes of irradiation. At 60, 90 and 120 minutes, the degradation percent was found to be 46%, 53%, 57%, and 58%, respectively. Finally, the degradation percent reached 58% at 150 minutes of irradiation. After 120 minutes of irradiation, degradation percentage did not significantly increase. Hence, 120 minutes of irradiation time was maintained for further experiments.

Effect of Dye Concentration

Figure 6 (d), a curve shows 63 % degradation when 5 mg/L MB was used. It may be due to the production of enough electron-hole pairs. When the dye concentration was increased, the degradation % seemed to be constantly decreasing. Nearly 57 % dye degradation was observed at 10 mg/L, while 42% dye degradation was found at 15 mg/L dye concentration. Further increase in MB concentration showed low percent degradation. It may be due to the low MB concentration acting upon the photocatalyst. Hence, 5 mg/L MB was selected for further experimentation.

Effect of pH on Dye Degradation

Figure 6 (c) displays the percent degradation of MB at different pH levels. One can see 27 % dye degradation at pH 4 and degradation % was found to be improved on increasing pH of solution. Maximum 70% degradation was attained at 10 pH. At higher pH values, the external surface of ZnO was negatively charged which draws cationic MB molecules due to electrostatic force of attraction. Hence, maximum removal occurred at higher pH values. The probable reason for the better photocatalytic degradation at higher pH may be due to the principle offered by -OH radical attack.

Photocatalytic Degradation of MB under Different Conditions

After optimizing all the parameters such as pH, catalyst dose, MB concentration, UV irradiation time, the photocatalytic efficiency of ZnO nanoparticles was studied in four conditions

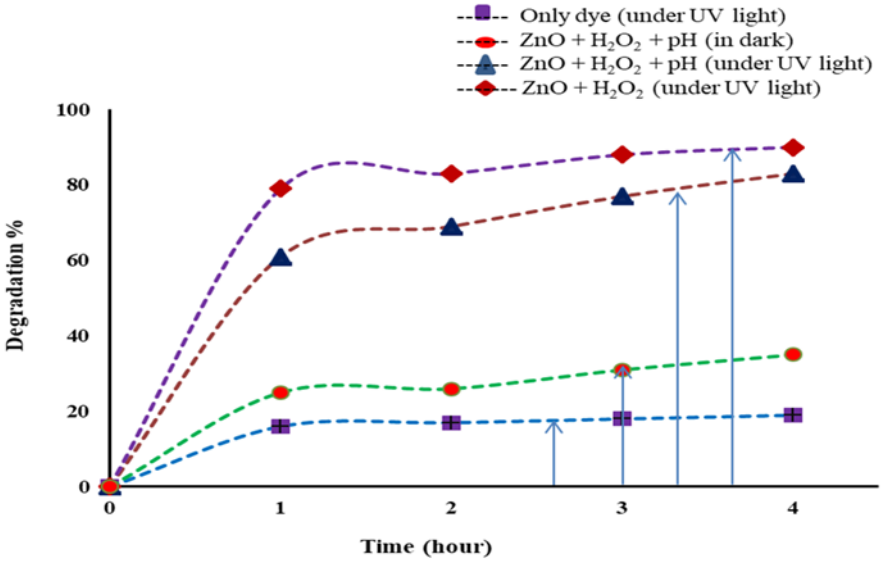

Figure 71. Photocatalytic degradation of MB under four conditions.

In Figure 7, blue curve represents percent degradation of MB in UV light irradiation without ZnO. Here, no significant degradation was observed. After one hour only 16 % degradation was observed. After one hour, very small increase in dye degradation was observed. After 4 hrs only 19 % degradation was perceived. Then, the condition was changed where MB was allowed to set at pH 10 in the presence of ZnO, H_2O_2 in dark for 4 hrs. Then degradation % was calculated and displayed as green curve in Figure 7. Here removal of MB was due to adsorption rather than degradation as it is in absence of light. Adsorption appears from the beginning and continuous up to 4 hrs. Here, only 35 % of MB appears to be adsorbed. Similarly, the brown curve represents percent degradation of MB with ZnO along with H_2O_2 under UV light. Here, pH was not maintained in the system. Results revealed that there is 83 % degradation was observed within 4 hrs. It is significantly high. Again, in order to increase percent degradation, pH 10 was maintained and UV light was irradiated. The results are displayed as purple curve. Here, 90 % degradation of MB could be seen within 4 hrs of UV irradiation when H_2O_2, along with ZnO photocatalyst, has been used in basic conditions. In this experiment, the H_2O_2 and pH successively activate ZnO and trigger the photocatalytic process. It may be due to the production of excess $^{\bullet}OH$ radicals from H_2O_2, as well as from basic medium of solution that helps to degrade MB.

In case of Cu-ZnO, the percentage dye degradation was significantly increased up to 98% which is shown in Figure 8 red curve. It is also compared with an experiment carried out in same condition along with ZnO which is exposed by green line in Figure 8.

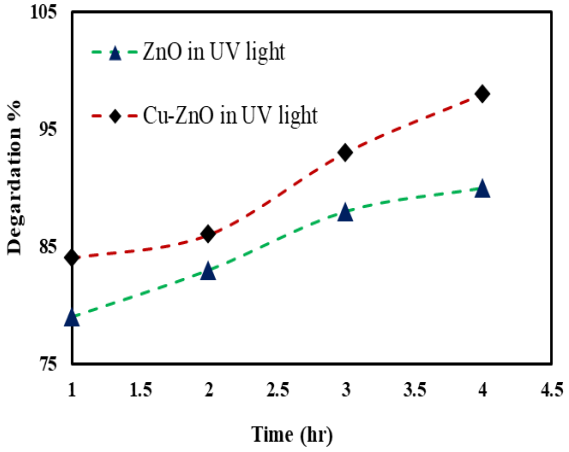

Figure 8. Photocatalytic degradation using ZnO and Cu-ZnO NPs in UV light.

Therefore, it is perceived that the MB degradation was upgraded by doping copper metal on zinc oxide. Various reports are in agreement with this finding (Rezapour *et al*., 2011; Okamoto *et al*., 1985; Fu *et al*., 2011; Kuriakose *et al*., 2015; Al-Mamun *et al*., 2023). It is supposed that the doping of metal creates an intermediate energy level which may increase the transport of electrons. Due to transference of electrons, recombination of electron-hole pair is controlled. A comparative study of the activity of as-prepared ZnO and Cu-ZnO nanocomposite with previously reported photocatalysts for the deprivation of dye is presented in Table 1.

Table 1. Comparison of ZnO nanoparticles and Cu-ZnO nanocomposite photocatalysts with previously reported photocatalysts.

Photocatalyst	Concentration of dye (mg/L)	Catalytical dose (mg)	Irradiation time (minutes)	Degradation %	References
Cu NPs	10	10	120	90	(Mali *et al*., 2020)
ZnO- NPs	10	-	140	43	(Vallejo *et al*.,
ZnO- NPs	10	-	140	63	2020b)
Cu-ZnO NPs	5	50	120	94	(Khalid *et al*., 2022)
Ag-ZnO NPs	-	100	60	73	(Blaženka *et al*.,2022)
Cu-ZnO NPs	-	20	180	60	(Shah *et al*., 2020)
ZnO NPs	5	30	240	90	Present study
Cu-ZnO NPs	5	30	240	98	

As can be seen in Table 1, MB degradation has been widely studied with the use of different photocatalysts. Metal oxides showed around 90% MB dye degradation. Metal-doped catalysts, showed improved photocatalytic performance. As compared to these composite photocatalysts, as prepared copper-doped zinc oxide photocatalyst showed 98% MB degradation.

Results revealed that the photocatalytic degradation performance of ZnO nanoparticles can be enhanced by altering surface area by doping transition metals. Cu is an important metal for doping since it is a member of the transition metal family having high electrical conductivity, and has the same radius as Zn (Sajjad *et al*., 2018). Besides this, its d-electrons may easily overlap with the ZnO valence band (Ijaz *et al*., 2017). Doping Cu into ZnO also increases their surface area and decreases their size, this results in improved photocatalytic processes (Tee *et al*., 2015). It improves the crystal defects as well and also affects the photosensitive characteristics by shifting the absorption band in the direction of the solar region when the photocatalytic degradation is analyzed through UV and visible region (Shanmugam *et al*., 2018). Cu has got several benefits such as low cost, high electronegativity than zinc, equivalent atomic size with zinc, and improved doping efficiency.

Proposed Photocatalytic Mechanism

ZnO is an inorganic semiconductor and is a heterogeneous photocatalyst. Upon irradiation with light, electrons are generated in the conduction band (CB) and holes are generated in the valence band (VB). Thus, produced electrons counter with adsorbed oxygen on the ZnO catalyst to give $O_2^{\bullet-}$ radical anions and the water from the solution combines with the holes to produce $^{\bullet}OH$ radicals. These $^{\bullet}OH$ undergoes the oxidation and reduction reaction while reacting with MB. These active classes are mainly accountable for the deprivation of MB. There are equal chances of recombination of electron-hole pairs. In this case, dopant Cu played a role in minimizing the recombination of electron-hole and sinking the band gap where transfer of electrons is possible. A schematic representation of photocatalytic degradation of dye using Cu doped ZnO is revealed in Figure 9.

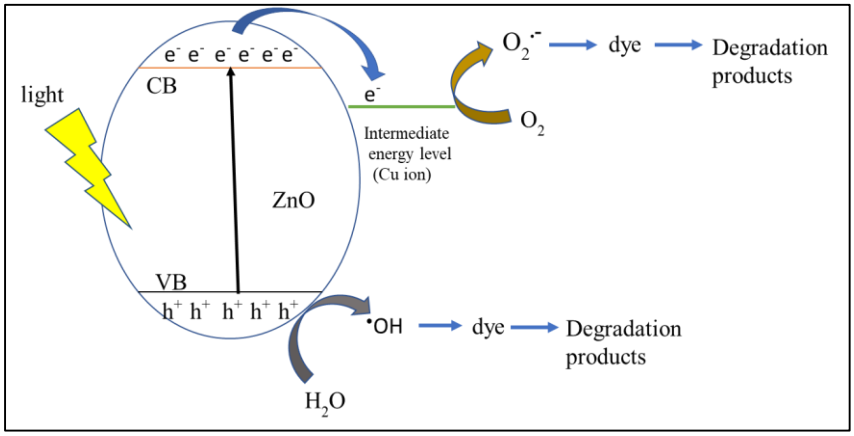

Figure 9. Schematic diagram of photocatalytic activity of Cu-ZnO nanocomposites for the degradation of dye.

The probable mechanism of photocatalytic degradation of MB dye pollutant using Cu-ZnO nanocomposites can be given as follows (Karthik, *et al*., 2022):

$(Cu\text{-}ZnO) + h\nu \rightarrow h^+ + e^-$ …. (3)

$e^- + O_2 \rightarrow (Cu\text{-}ZnO) + {}^{\bullet}O_2^-$ … (4)

$h^+ + H_2O \rightarrow {}^{\bullet}OH + H^+$ … (5)

$OH^- + h^+ \rightarrow {}^{\cdot}OH$ … (6)

$H_2O_2 + {}^{\bullet}O_2^- \rightarrow {}^{\bullet}OH + OH^- + O_2$ … (7)

$H_2O_2 + h\nu \rightarrow 2{}^{\bullet}OH$ … (8)

$^{\bullet}OH$ + MB dye pollutant $\rightarrow CO_2 + H_2O$ … (9)

$^{\bullet}O_2^-$ + MB dye pollutant $\rightarrow CO_2 + H_2O$ … (10)

CONCLUSIONS

UV-active ZnO nanoparticles and Cu-ZnO nanocomposite photocatalysts can be synthesized by green route using leaves of *Cinnamomum camphora* where the components present in leaves act as a capping agent to control the overgrowth. XRD pattern showed the crystalline phase of ZnO and Cu-ZnO having 21 and 17.51 nm crystallite size, respectively. SEM images showed rounded shaped nanoparticles and UV-visible spectrophotometry displayed characteristic absorption bands of ZnO at 378 nm and

Cu-ZnO at 382 nm. ZnO showed 90% MB dye degradation while Cu-ZnO photocatalyst showed 98% MB degradation at pH 10 using 30 mg catalyst dose. Results exposed that the photocatalytic degradation performance of ZnO can be enhanced by altering surface area by doping transition metals like Cu.

ACKNOWLEDGMENTS

Authors are thankful to Nepal Academy of Science and Technology (NAST), Nepal for XRD and Dr. Mahesh Joshi for SEM.

AUTHOR CONTRIBUTION

Conceptualization: PP; Investigation: AN, PP; Methodology: PP; Data curation: AN; Data analysis: AN; Writing - original draft: PP; Writing - review and editing: AN.

CONFLICT OF INTEREST

The authors do not have any conflicts of interest throughout this research work.

DATA AVAILABILITY STATEMENT

The data supporting this study's findings are available from the corresponding authors upon reasonable request.

REFERENCES

Alharthi, F.A., Alghamdi, A.A., Alothman, A.A., Almarhoon, Z.M., Alsulaiman, M.F., & Al-Zaqri, N. (2020). Green synthesis of ZnO nanostructures using *Salvadora persica* leaf extract: applications for photocatalytic degradation of methylene blue dye. *Crystals*, *10*(6), 441. https://doi.org/10.3390/cryst10060441.

Al-Mamun, Md.R., Iqbal Rokon, Md. Z., Rahim, Md.A., Hossain, Md.I., Islam, Md.S., Ali, Md. R., Bacchu, M.S., Waizumi, H., Komeda, T., & Hossain Khan, M.Z. (2023). Enhanced photocatalytic activity of Cu and Ni-doped ZnO nanostructures: A comparative study of methyl orange dye degradation in aqueous solution. *Heliyon*, *9*(6), e16506. https://doi.org/10.1016/j.heliyon.2023.e16506.

Ashwini, J., Aswathy, T.R., Rahul, A.B., Thara, G.M., & Nair, A.S. (2021). Synthesis and characterization of zinc oxide nanoparticles using *Acacia caesi*a bark extract and its photocatalytic and antimicrobial activities. *Catalysts*, *11*(12), 1507. https://doi.org/10.3390/catal11121507.

Bhuyan, T., Mishra, K., Khanuja, M., Prasad, R., & Varma, A. (2015). Biosynthesis of zinc oxide nanoparticles from *Azadirachta indica* for antibacterial and photocatalytic applications. *Materials Science in Semiconductor Processing*, *32*, 55–61. https://doi.org/10.1016/j.mssp.2014.12.053.

Blažeka, D., Radičić, R., Maletić, D., Živković, S., Momčilović, M., & Krstulović, N. (2022). Enhancement of methylene blue photodegradation rate using laser synthesized Ag-doped ZnO nanoparticles. *Nanomaterials*, *12*(15), 2677. https://doi.org/10.3390/nano12152677.

Bratovcic, A. (2019). Different applications of nanomaterials and their impact on the environment. *International Journal of Material Science and Engineering*, *5*(1), 1–7. https://doi.org/10.14445/23948884/IJMSE-V5I1P101.

Cai, Z., Sun, Y., Liu, W., Pan, F., Sun, P., & Fu, J. (2017). An overview of nanomaterials applied for removing dyes from wastewater. *Environmental Science and Pollution Research*, *24*(19), 15882–15904. https://doi.org/10.1007/s11356-017-9003-8.

Davar, F., Majedi, A., & Mirzaei, A. (2015). Green synthesis of zno nanoparticles and its application in the degradation of some dyes. *Journal of the American Ceramic Society*, *98*(6), 1739–1746. https://doi.org/10.1111/jace.13467.

Fu, M., Li, Y., Wu, S., Lu, P., Liu, J., & Dong, F. (2011). Sol–gel preparation and enhanced photocatalytic performance of Cu-doped ZnO nanoparticles. *Applied Surface Science*, *258*(4), 1587–1591. https://doi.org/10.1016/j.apsusc.2011.10.003.

Gaurav, A., Beura, R., Kumar, J.S., & Thangadurai, P. (2019). Study on the effect of copper ion doping in zinc oxide nanomaterials for photocatalytic applications. *Materials Chemistry and Physics*, *230*, 162–171. https://doi.org/10.1016/j.matchemphys.2019.03.056.

Ghosh A., Kumari N. & Bhattachrjee A. (2015). Influence of Cu doping on structural, electrical and optical properties of ZnO. *Pramana, 84(4)*, 621-635. https://doi.org/10.1007/s12043-014-0851-1.

Hussein, F. H., & Halbus, A. F. (2012). Rapid Decolorization of Cobalamin. *International Journal of Photoenergy*, *2012,* 495435. https://doi.org/10.1155/2012/495435.

Ijaz, F., Shahid, S., Khan, S.A., Ahmad, W., & Zaman, S. (2017). Green synthesis of copper oxide nanoparticles using *Abutilon indicum* leaf extract: Antimicrobial, antioxidant and photocatalytic dye degradation activitie. *Tropical Journal of Pharmaceutical Research*, *16*(4), 743. https://doi.org/10.4314/tjpr.v16i4.2.

Karthik, K.V., Raghu, A.V., Reddy, K.R., Ravishankar, R., Sangeeta, M., Shetti, N.P., & Reddy, C.V. (2022). Green synthesis of Cu-doped ZnO nanoparticles and its application for the photocatalytic degradation of hazardous organic pollutants. *Chemosphere*, *287*, 132081. https://doi.org/10.1016/j.chemosphere.2021.132081.

Khalid, A., Ahmad, P., Khan, A., Muhammad, S., Khandaker, M.U., Alam, Md. M., Asim, M., Din, I.U., Chaudhary, R.G., Kumar, D., Sharma, R., Faruque, M.R.I., & Emran, T.B. (2022). Effect of Cu doping on ZnO nanoparticles as a photocatalyst for the removal of organic wastewater. *Bioinorganic Chemistry and Applications*, *2022*, 1–12. https://doi.org/10.1155/2022/9459886.

Khan, I., Saeed, K., Zekker, I., Zhang, B., Hendi, A.H., Ahmad, A., Ahmad, S., Zada, N., Ahmad, H., Shah, L.A., Shah, T., & Khan, I. (2022). Review on methylene blue: its properties, uses, toxicity and photodegradation. *Water*, *14*(2), 242. https://doi.org/10.3390/w14020242.

Khan, S. A., Noreen, F., Kanwal, S., Iqbal, A., & Hussain, G. (2018). Green synthesis of ZnO and Cu-doped ZnO nanoparticles from leaf extracts of *Abutilon indicum*, *Clerodendrum infortunatum, Clerodendrum inerme* and investigation of their biological and photocatalytic activities. *Materials Science and Engineering: C*, *82*, 46–59. https://doi.org/10.1016/j.msec.2017.08.071.

Koutavarapu, R., Babu, B., Reddy, C.V., Reddy, I.N., Reddy, K.R., Rao, M.C., Aminabhavi, T. M., Cho, M., Kim, D., & Shim, J. (2020). ZnO nanosheets-decorated Bi_2WO_6 nanolayers as efficient photocatalysts for the removal of toxic environmental pollutants and photoelectrochemical solar water oxidation. *Journal of Environmental Management*, *265*, 110504. https://doi.org/10.1016/j.jenvman.2020.110504

Kuriakose, S., Satpati, B., & Mohapatra, S. (2015). Highly efficient photocatalytic degradation of organic dyes by Cu doped ZnO nanostructures. *Physical Chemistry Chemical Physics*, *17*(38), 25172–25181. https://doi.org/10.1039/C5CP01681A.

Malarkodi, C., Rajeshkumar, S., Paulkumar, K., Vanaja, M., Gnanajobitha, G., & Annadurai, G. (2014). Biosynthesis and Antimicrobial Activity of Semiconductor Nanoparticles against Oral Pathogens. *Bioinorganic Chemistry and Applications*, *2014*, 347167. https://doi.org/10.1155/2014/347167.

Mali, S.C., Dhaka, A., Githala, C.K., & Trivedi, R. (2020). Green synthesis of copper nanoparticles using *Celastrus paniculatus* Willd. Leaf extract and their photocatalytic and antifungal properties. *Biotechnology Reports*, *27*, e00518. https://doi.org/10.1016/j.btre.2020.e00518.

Modwi, A., Ghanem, M.A., Al-Mayouf, A.M., & Houas, A. (2018). Lowering energy band gap and enhancing photocatalytic properties of Cu/ZnO composite decorated by transition metals. *Journal of Molecular Structure*, *1173*, 1–6. https://doi.org/10.1016/j.molstruc.2018.06.082.

Okamoto, K., Yamamoto, Y., Tanaka, H., Tanaka, M., & Itaya, A. (1985). Heterogeneous photocatalytic decomposition of phenol over TiO_2 powder. *Bulletin of the Chemical Society of Japan*, *58*(7), 2015–2022. https://doi.org/10.1246/bcsj.58.2015.

Ramsay, R.R., Dunford, C., & Gillman, P.K. (2007). Methylene blue and serotonin toxicity: Inhibition of monoamine oxidase A (MAO A) confirms a theoretical prediction. *British Journal of Pharmacology*, *152*(6), 946. https://doi.org/10.1038/sj.bjp.0707430.

Rezapour, M., & Talebian, N. (2011). Comparison of structural, optical properties and photocatalytic activity of ZnO with different morphologies: Effect of synthesis methods and reaction media. *Materials Chemistry and Physics*, *129*(1–2), 249–255. https://doi.org/10.1016/j.matchemphys.2011.04.012.

Sahu, S., Pahi, S., Sahu, J.K., Sahu, U.K., & Patel, R.K. (2020). Kendu (*Diospyros melanoxylon* Roxb) fruit peel activated carbon-an efficient bioadsorbent for methylene blue dye: Equilibrium, kinetic, and thermodynamic study. *Environmental Science and Pollution Research*, *27*(18), 22579–22592. https://doi.org/10.1007/s11356-020-08561-2.

Sajjad, M., Ullah, I., Khan, M.I., Khan, J., Khan, M.Y., & Qureshi, M.T. (2018). Structural and optical properties of pure and copper doped zinc oxide nanoparticles. *Results in Physics*, *9*, 1301–1309. https://doi.org/10.1016/j.rinp.2018.04.010.

Shah, A.A., Bhatti, M.A., Tahira, A., Chandio, A.D., Channa, I.A., Sahito, A.G., Chalangar, E., Willander, M., Nur, O., & Ibupoto, Z.H. (2020). Facile synthesis of copper doped ZnO nanorods for the efficient photo degradation of methylene blue and methyl orange. *Ceramics International*, *46*(8), 9997–10005. https://doi.org/10.1016/j.ceramint.2019.12.024.

Shanmugam, V., & Jeyaperumal, K.S. (2018). Investigations of visible light driven Sn and Cu doped ZnO hybrid nanoparticles for

photocatalytic performance and antibacterial activity. *Applied Surface Science*, *449*, 617–630. https://doi.org/10.1016/j.apsusc.2017.11.167.

Suwanboon, S., Amornpitoksuk, P., Sukolrat, A., & Muensit, N. (2013). Optical and photocatalytic properties of La-doped ZnO nanoparticles prepared via precipitation and mechanical milling method. *Ceramics International*, *39*(3), 2811–2819. https://doi.org/10.1016/j.ceramint.2012.09.050

Tee, S.Y., Ye, E., Pan, P.H., Lee, C. J.J., Hui, H.K., Zhang, S.-Y., Koh, L.D., Dong, Z., & Han, M.-Y. (2015). Fabrication of bimetallic Cu/Au nanotubes and their sensitive, selective, reproducible and reusable electrochemical sensing of glucose. *Nanoscale*, *7*(25), 11190–11198. https://doi.org/10.1039/C5NR02399H.

Vallejo, W., Cantillo, A., Salazar, B., Diaz-Uribe, C., Ramos, W., Romero, E., & Hurtado, M. (2020). Comparative study of ZnO thin films doped with transition metals (Cu and Co) for methylene blue photodegradation under visible irradiation. *Catalysts*, *10*(5), 528. https://doi.org/10.3390/catal10050528.

Viorica, G.P., Musat, V., Pimentel, A., Calmeiro, T.R., Carlos, E., Baroiu, L., Martins, R., & Fortunato, E. (2019). Hybrid (Ag)ZnO/Cs/PMMA nanocomposite thin films. *Journal of Alloys and Compounds*, *803*, 922–933. https://doi.org/10.1016/j.jallcom.2019.06.373.

Xu, L., Zhou, Y., Wu, Z., Zheng, G., He, J., & Zhou, Y. (2017). Improved photocatalytic activity of nanocrystalline ZnO by coupling with CuO. *Journal of Physics and Chemistry of Solids*, *106*, 29–36. https://doi.org/10.1016/j.jpcs.2017.03.001

Yusof A.S., Hassan Z. (2018). Fabrication and characterization of Cu doped ZnO filmsusinf RF reactive magnatron sputtering. *Journal of Physics conference series, 1083(1)*, 012062 https://doi.org/10.1088/1742-6596/1083/1/012062.